Combined microtomography, thermal desorption spectroscopy, X-ray diffraction study of hydrogen trapping behavior in 7XXX aluminum alloys

Bhuiyan, Md. Shahnewaz
Department of Mechanical Engineering, Kyushu University

Toda, Hiroyuki
Department of Mechanical Engineering, Kyushu University

Peng, Zhang
Department of Mechanical Engineering, Kyushu University

Hang, Su
Department of Mechanical Engineering, Kyushu University

他

出版情報：Materials Science and Engineering : A. 655, pp.221-228, 2016-02-08
バージョン：
権利関係：

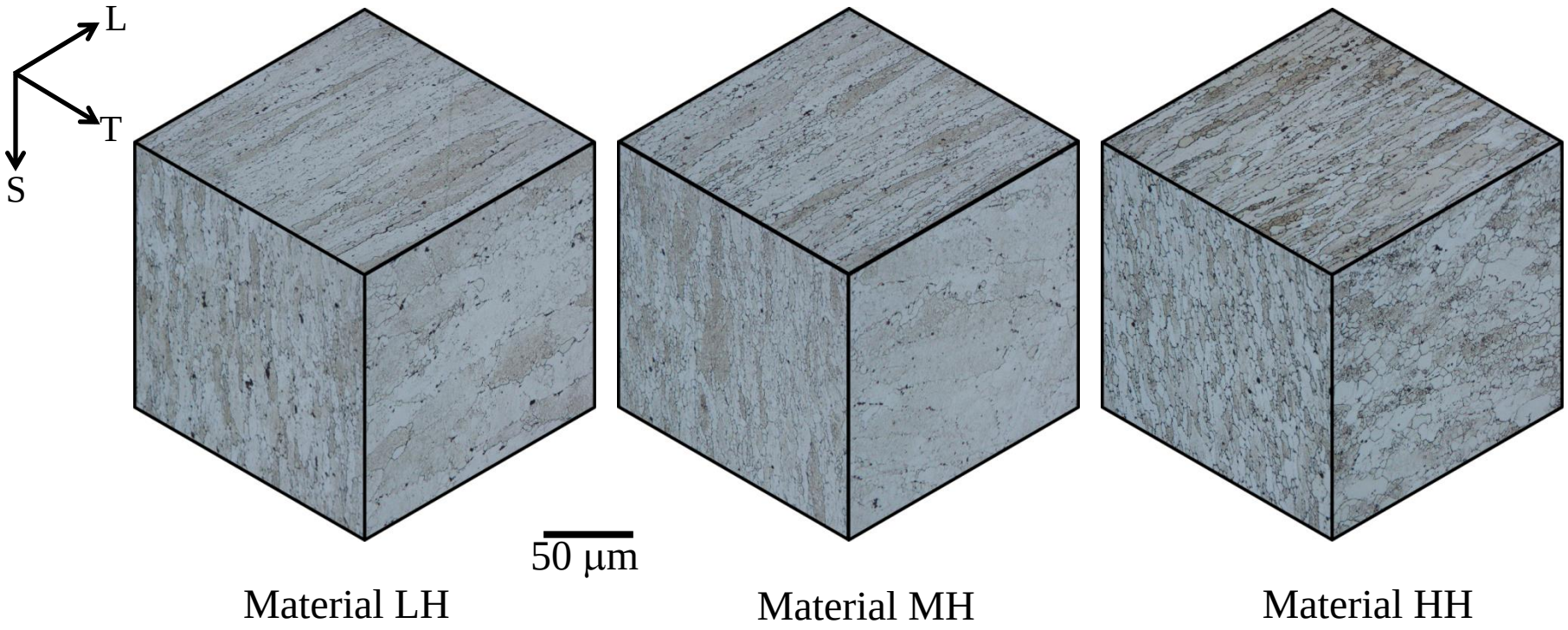

Fig. 1. Optical micrograph of the alloys investigated.

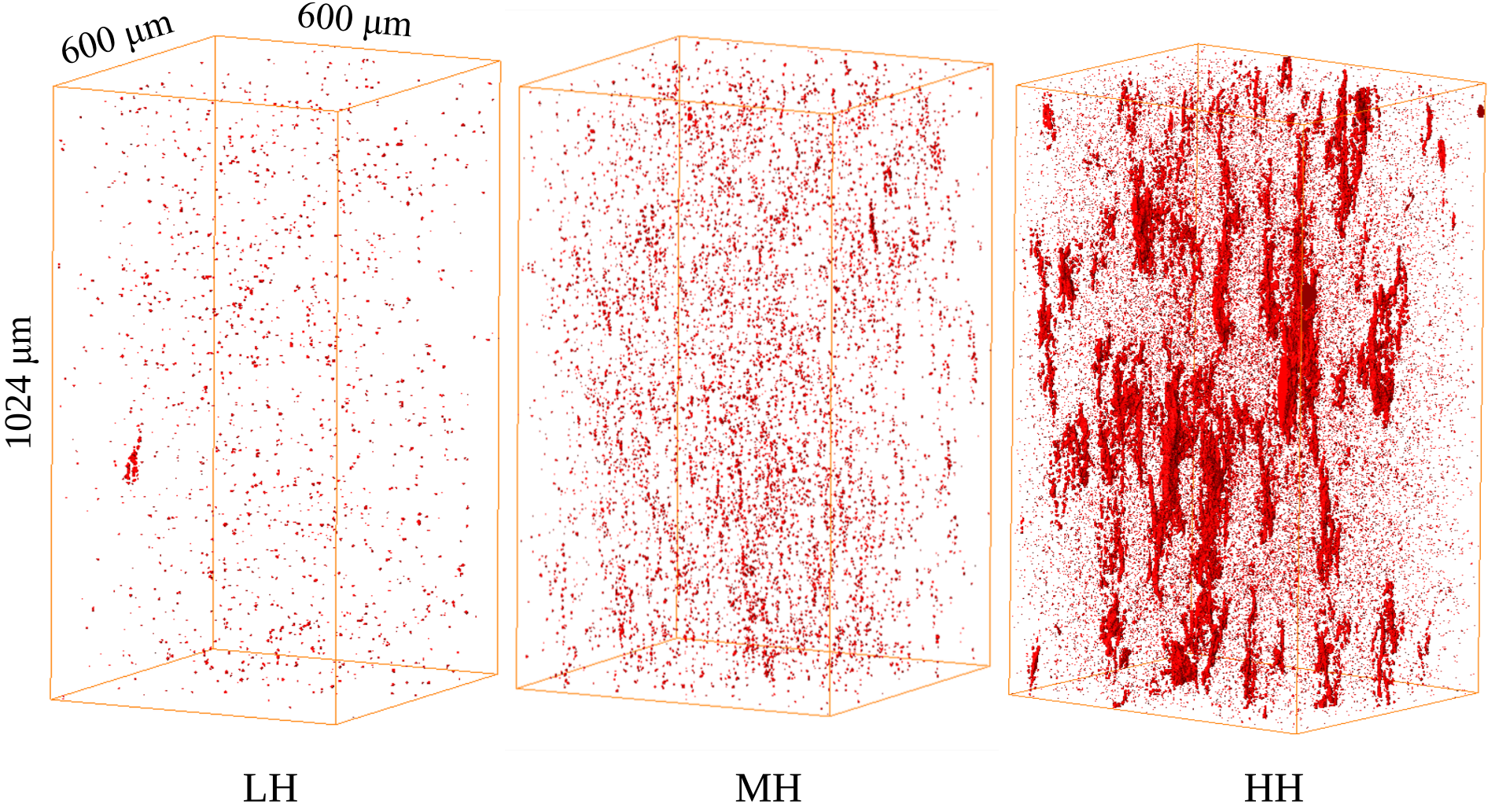

Fig. 2. 3D perspective views of micropores. Only micropores were extracted and shown here, and underlying aluminum is not displayed.

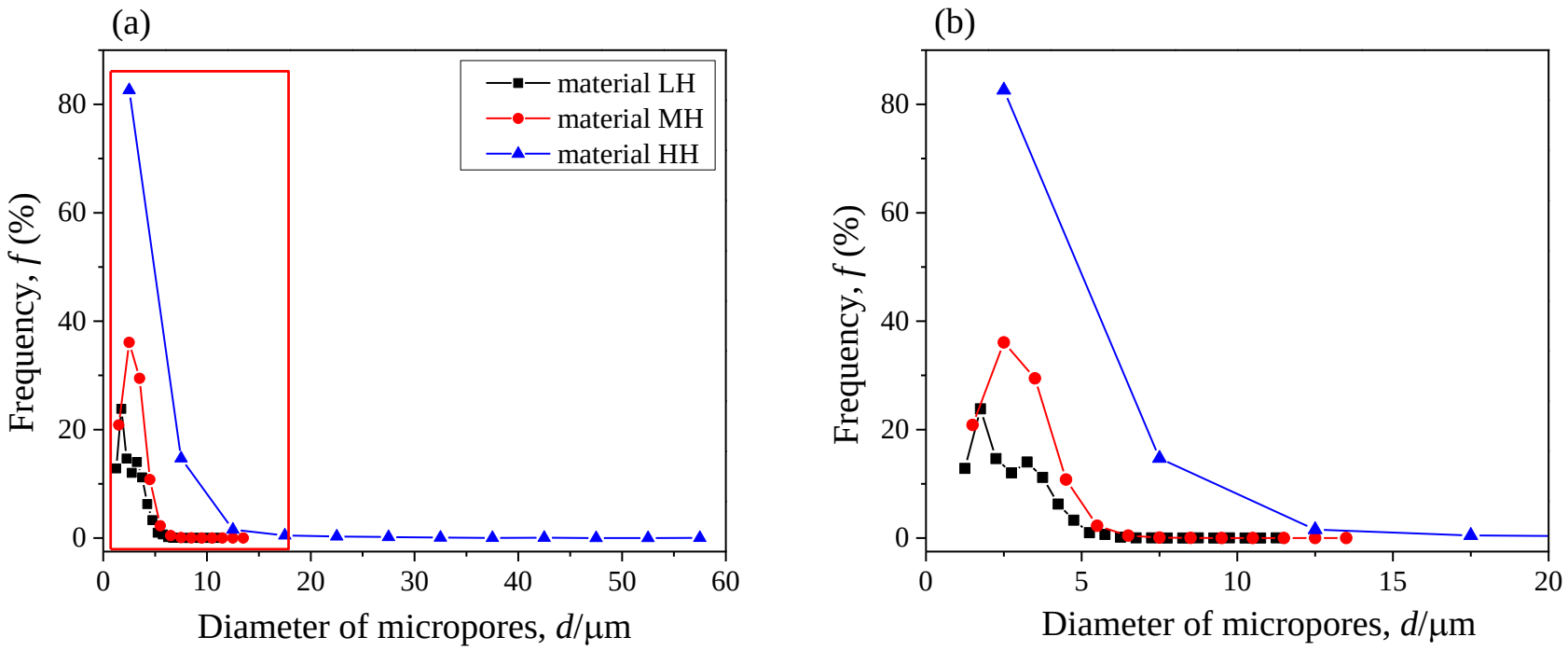

Fig. 3 (a) Size distributions of micropores in material LH, material MH and material HH, and (b) magnified view of Fig. (a) labeled by red rectangle.

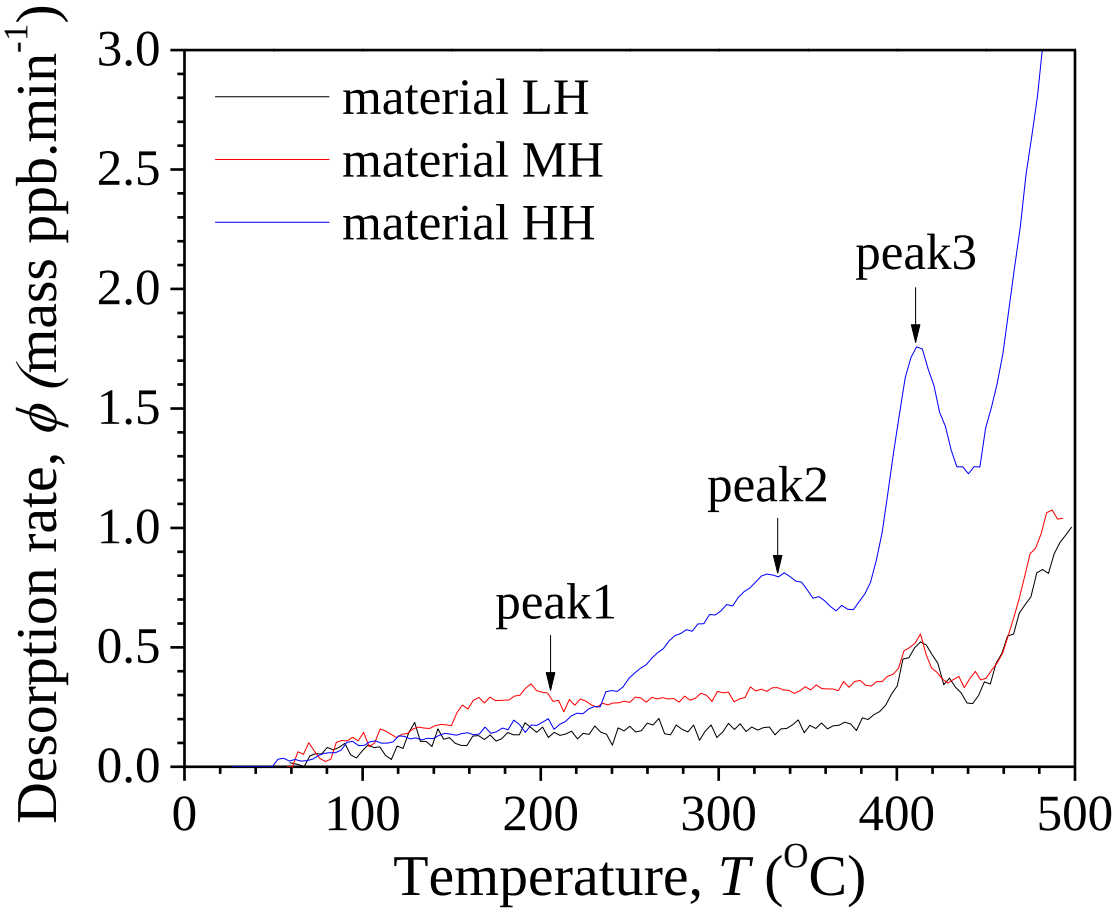

Fig. 4 Thermal Desorption Spectra of material LH (black line), material MH (red line), and material HH (blue line), respectively at a heating rate of 100 ^{O}C/h.

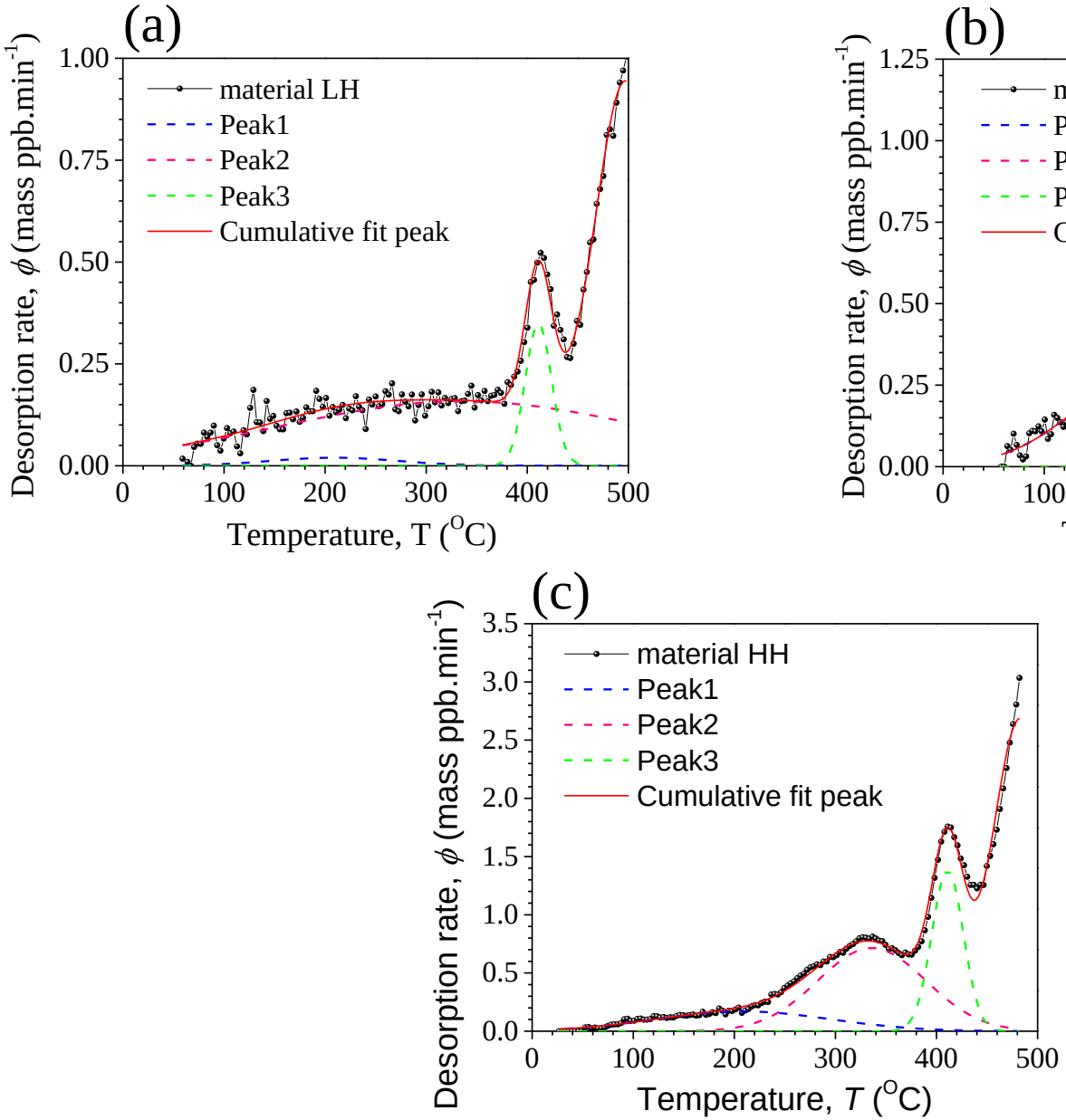

Fig. 5 Measured Thermal Desorption Spectra and fitted curve using Gaussian fit of material LH (a), material MH (b), and material HH (c), respectively at a heating rate of 100 ^{O}C/h.

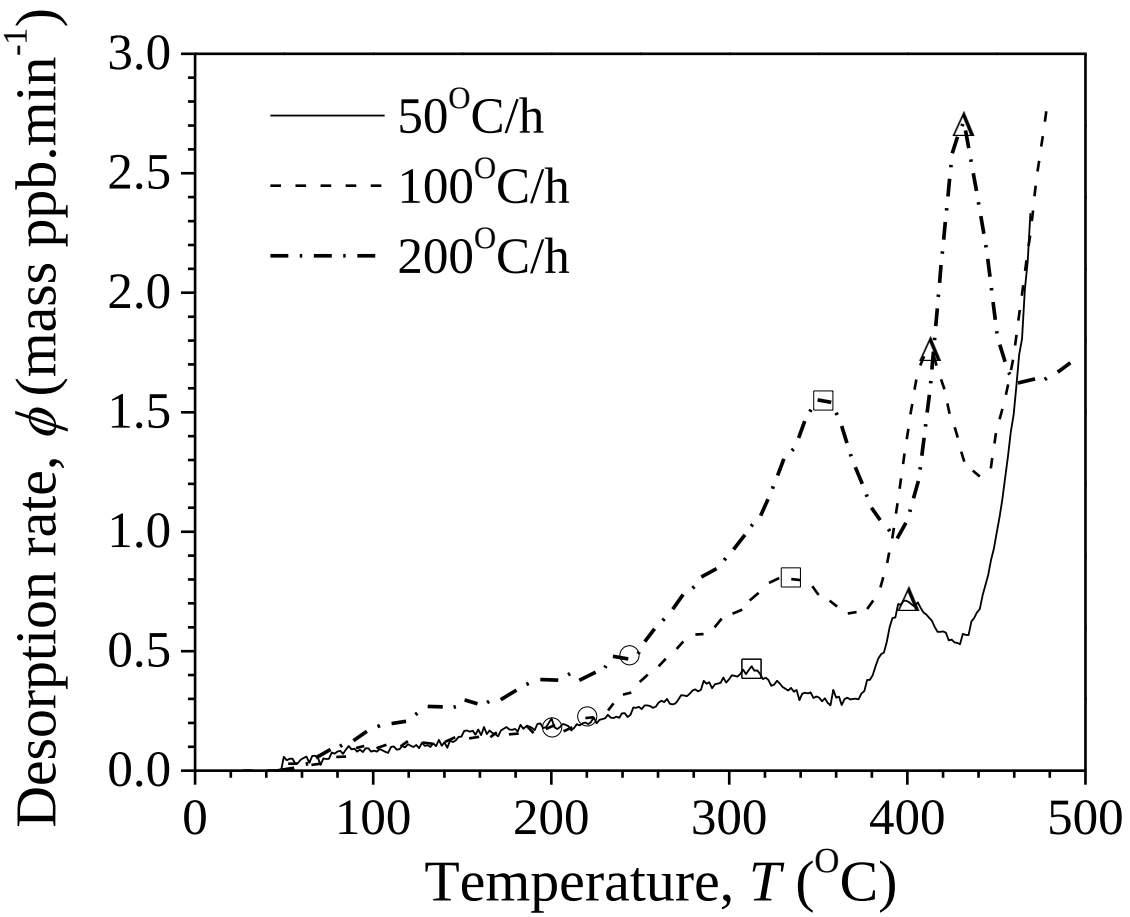

Fig. 6 Thermal desorption spectra of material HH at different heating rates. The location of peak1, peak2 and peak3 is indicated with □, ○, and Δ, respectively

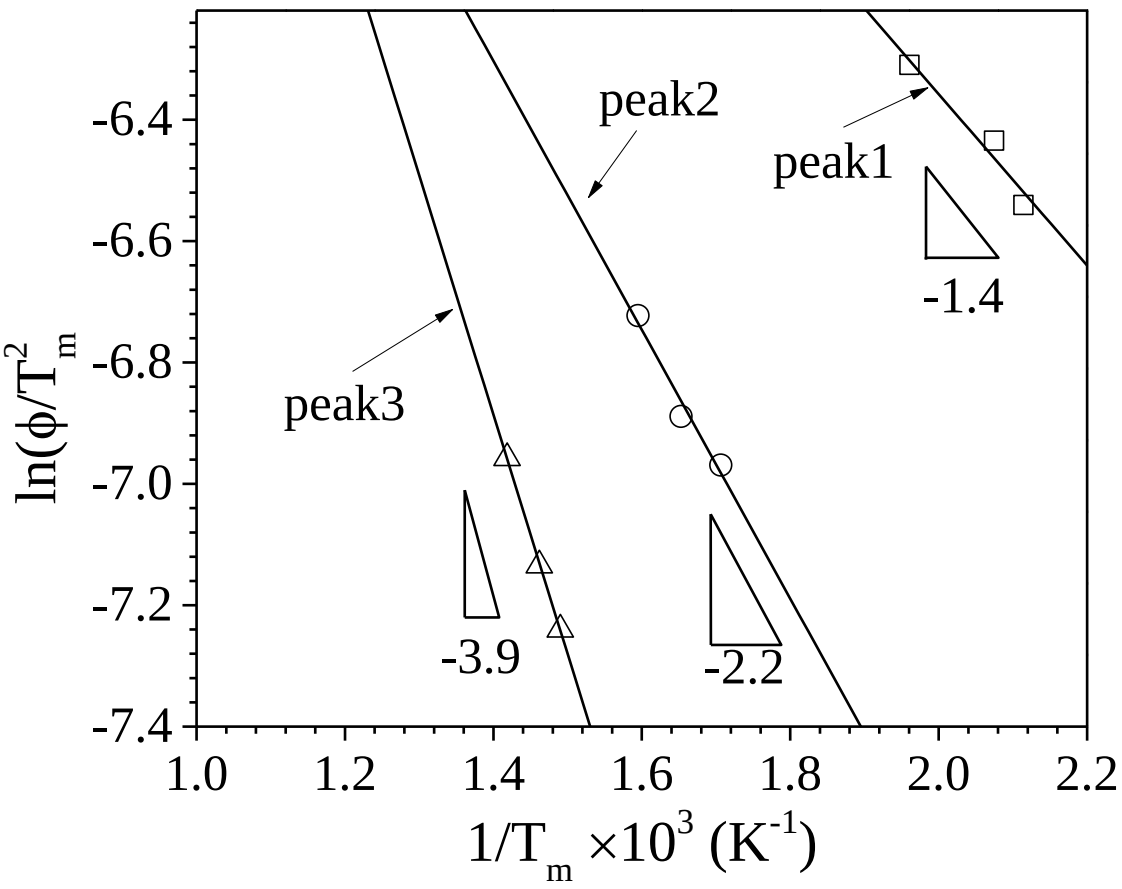

Fig. 7 Relationship between ln $\left(\frac{\varphi}{T_2^2}\right)$ and $^1/_{T_m}$ corresponding to Fig. 3.

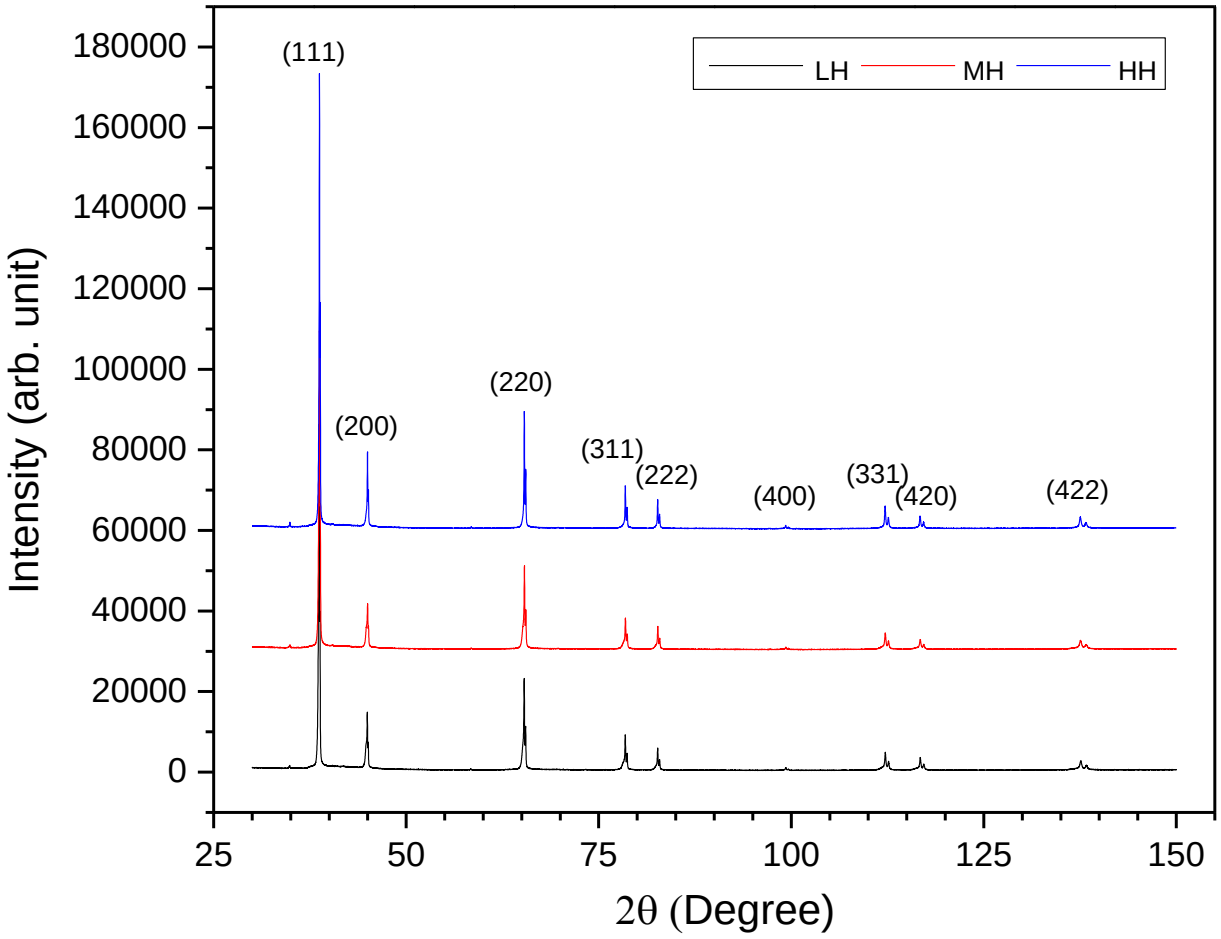

Fig. 8 X-ray diffractograms of material LH (black line), material MH (red line), and material HH (blue line), respectively.

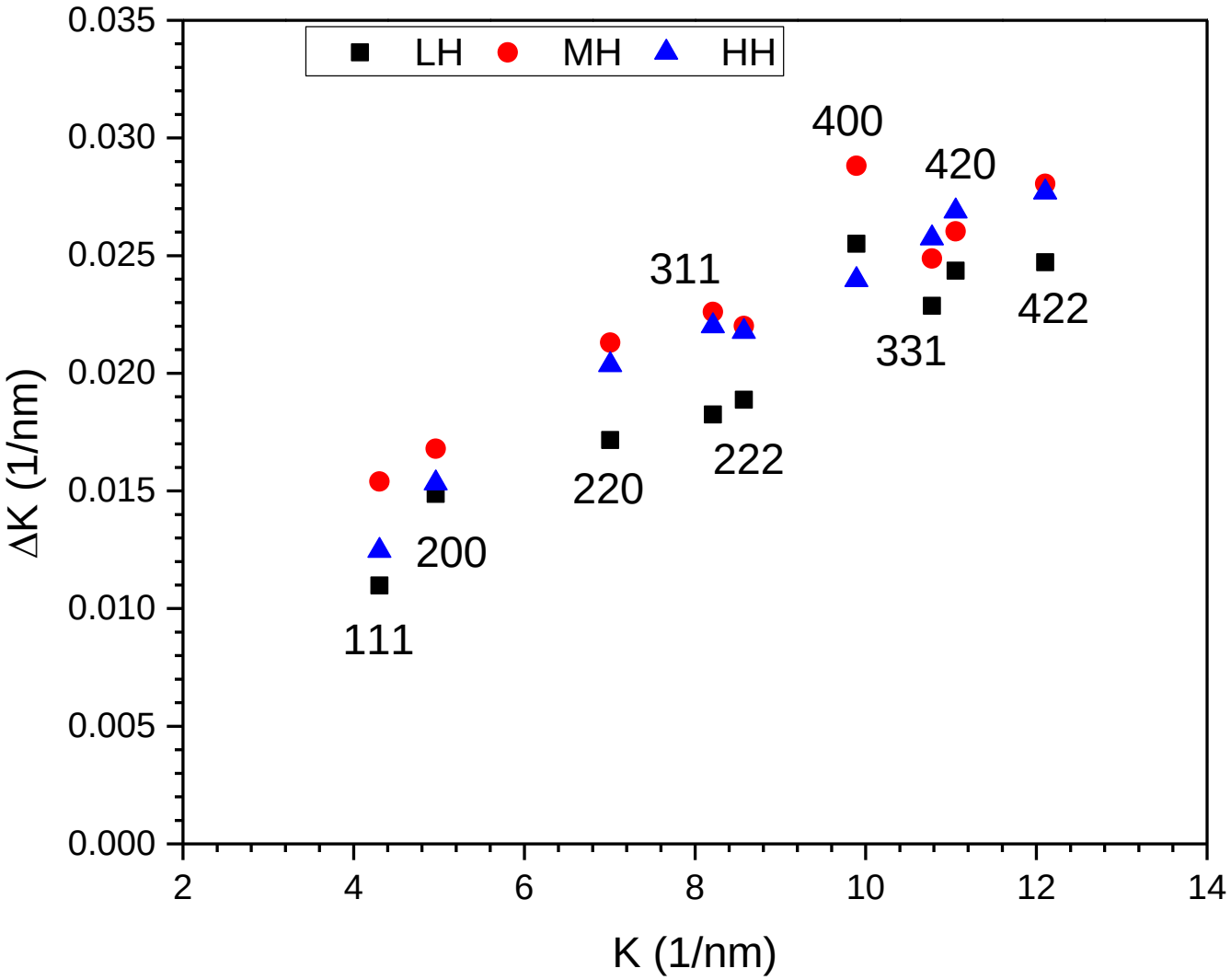

Fig. 9 The FWHM as a function of *K*, classical Williamson-Hall plot.

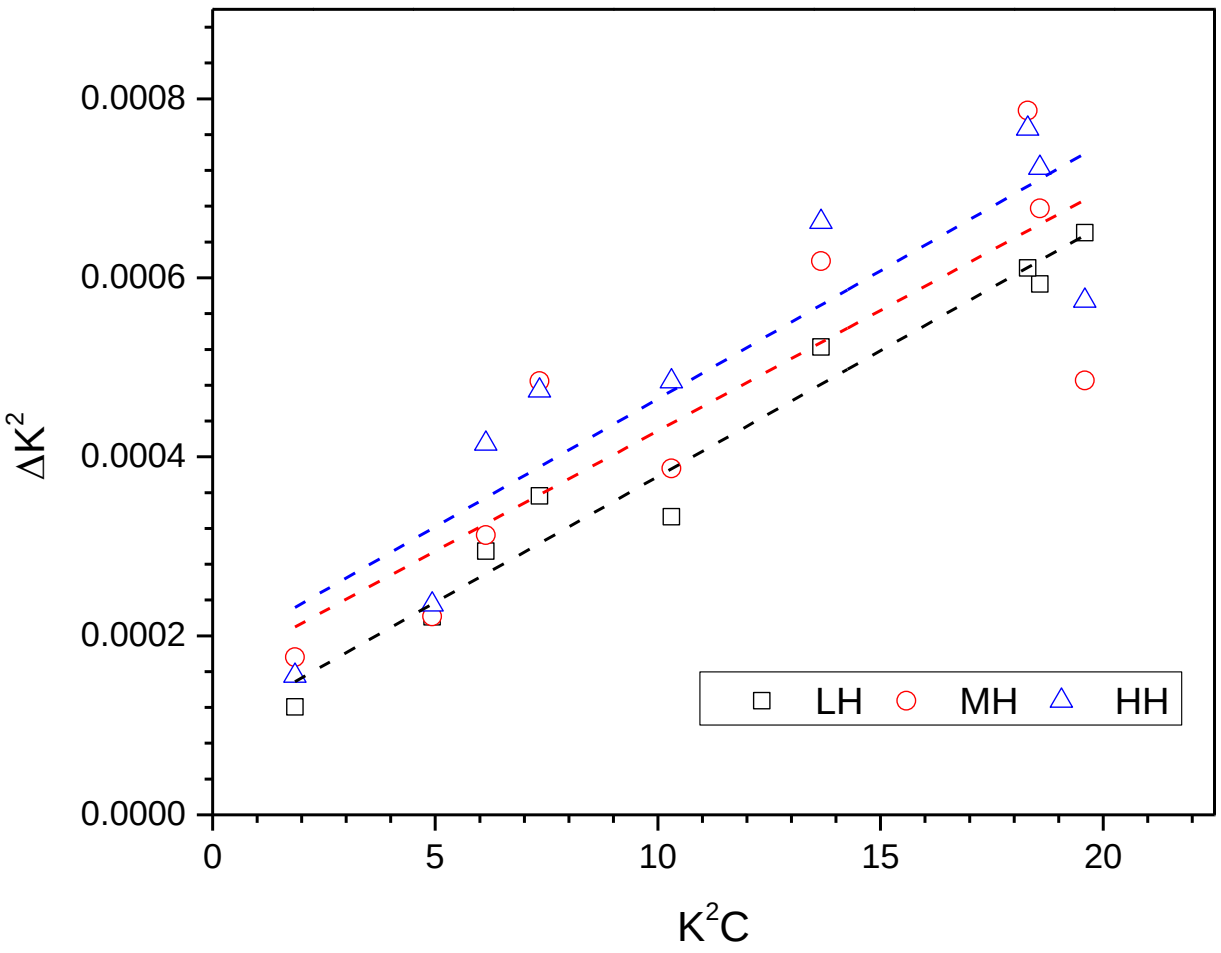

Fig. 10 Peak broadening analysis using the modified Williamson-Hall plot of material LH (black line), material MH (red line), and material HH (blue line), respectively.